EXPERIMENTAL RESULTS OF DOUBLE DISPERSIVE LONGITUDINAL PROPAGATION IN A "DUMILOAD" ROD FOR SONAR TRANSDUCER TESTING

Fernando L. de Magalhães, fermag@technologist.com
Sonar Group - Brazilian Navy Research Institute (IPqM)
R. Ipiru, 02 – Ilha do Governador – RJ - Brazil

Moysés Zindeluk, moyses@ufrj.br
PEM/COPPE - Federal University of Rio de Janeiro (UFRJ)
Centro de Tecnologia – Bloco G – Cidade Universitária – RJ - Brazil

Abstract. *For low frequency and high power acoustical fields, calibration tests of sonar transducers are usually carried out in large water environments or, under more economical and controlled conditions, by applying in laboratory devices named "DUMILOADs" (Dummy Mechanical Impedance Loads). With the aim to overcome the operational restrictions concerning the DUMILOAD models published in the literature, a novel kind of mechanoacoustical load device, which uses a PMMA cylindrical rod coupled to the sensitive face of a piezoelectric sonar transducer, was recently developed by the authors. The device is designed to apply, in the air, an acoustic impedance similar to the radiation impedance in the water, when harmonic longitudinal waves are propagating in the rod. After modeling the superposition of geometric and material dispersive effects, which characterize non slender viscoelastic bars, four different loading devices were produced. From comparisons between analytical and experimental imitance curves, the good capacity of PMMA rods to acoustically simulate water is here demonstrated. Moreover, by using the strain waves monitored on the cylindrical surface of the propagation medium, the sound level of the testing transducer is obtained from an absolute calibration procedure as it was in the water. Based on the experimental results, the paper concludes about the importance of material-geometric dispersion data to correct phase and amplitude distortions of longitudinal waves in the rods and consequently to identify the force and the velocity responses on the transducer face from strain measurements along the DUMILOAD.*

Keywords *: longitudinal propagation, material dispersion, geometric dispersion, sonar transducer, DUMILOAD*

1. INTRODUCTION

Particularly for low frequency and high power underwater acoustic transducers, calibration processes and endurance tests are carried out in large water environments, where free field and high hydrostatic pressure conditions can be satisfied. In order to avoid the complexity and the high costs related to such kind of scenario, in laboratory test devices named DUMILOADs -Dummy Mechanical Impedance Loads- have been used by sonar transducers developers. Despite their good measuring accuracy up to the first tens of kilohertz, the two types of DUMILOAD described in the literature (Afonso and Magalhães, 1999) are dynamically unstable for long-term tests and restricted to narrow bandwidth applications. To overcome these limitations, the authors recently developed a novel type of mechanoacoustical load device named "Propagation Rod DUMILOAD", or "PRD", which uses a cylindrical rod made of polymethyl methacrylate (PMMA) as "hydroacoustic" impedance medium.

As depicted in Fig. 1, the PRD is designed to submit to a Tonpilz transducer (Xiping and Jing, 2009), in the air, an acoustic load similar to the hydroacoustic impedance, when longitudinal harmonic elastic waves are propagating in the rod. In an overview, the rod is configured by a long straight cylinder with two or more segments of different diameters and should be made of a material as close as possible to the water in terms of characteristic impedance. From the calibration interface, sinusoidal bursts are excited with carrier frequencies defined in the half-power transmission band of the transducer. In view that such nature of disturbances preserves the electroacoustic characteristics of the excitation source, by monitoring the strain signal along the loading rod the force and the velocity longitudinal fields are defined, leading to the calculation of the acoustic power and the sound level of the transducer. In case of a rod representing satisfactorily the acoustic characteristics of the water, the transmission response of the transducer can be directly obtained from an absolute calibration process. In this work, by using four rods with different propagating behaviors, experimental results concerning the acoustic calibration of a 51 kHz Tonpilz transducer (object transducer) are analyzed. The results point out to the good applicability of the PRD as an accurate and stable device for calibrating sonar projectors. It is also shown that it is feasible to measure the electrical imitance curves on the transducer terminals, under simulated acoustic radiation conditions, even adopting continuous excitation techniques in the PRD.

As indicated in the literature (Casem et al., 2003), although some types of strain sensors can be used to determine the force and velocity fields on the cylindrical surface of a bar (where the lateral inertia can be ignored) or rod (where displacements, strains, stresses, forces and velocities are taken in the longitudinal and radial directions), there are some uncertainties concerning the longitudinal propagation in viscoelastic 1-D and 3-D media. Besides the attenuation of the

disturbances, the propagation of multi-frequency acoustic waves in a bar leads to a dispersive behavior where the phase velocity increases with the frequency. The same is applicable to the attenuation factor. Moreover, when the wavelength is of the same order or smaller than the diameter, a bar behaves dynamically like a rod and the effects of another kind of dispersion, uniquely geometrical, become significant for longitudinal propagation. For a rod made of a purely elastic material the phase velocity decreases with increasing frequency, converging to specific levels modally defined. The superposition of the material and geometric dispersion effects yields a phase velocity increasing or decreasing with frequency, according to their relative importance and depending on the frequency band of the disturbance. As another important consequence of geometric dispersion, it is proved that a longitudinal wave, even when excited in an initially uniform condition, may experiment a non-planar transversal distribution while the disturbance moves along the rod (Tyas and Poppe, 2005). This type of distortion equally occurs for viscoelastic rods and it can be responsible for important uncertainties in the signal monitored by strain-gages, once the dynamic conditions on the rod surface do not necessarily represent the conditions at the inside particles. Thus, since the loading rods here treated are not perfectly slender propagation media, experimental aspects concerning double dispersive effects are also commented. The paper concludes about the existence of a cut-off frequency of the measuring process in the PRDs.
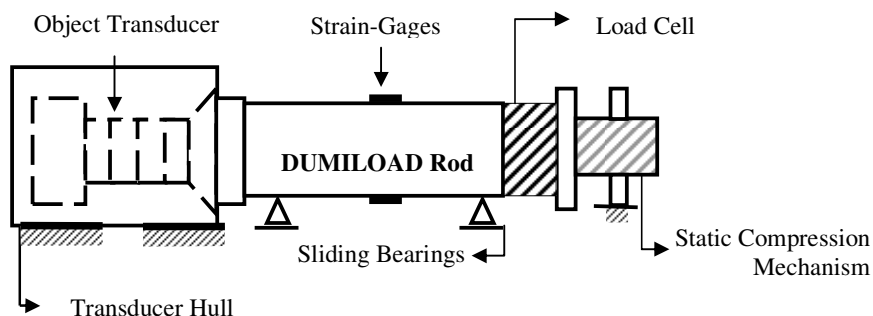

Figure 1. Schematic drawing of the "Propagation Rod DUMILOAD" (PRD).

2. DESIGNING OF DUMMY LOAD RODS

Due to the dynamic equivalency between acoustical and electrical transmission lines, when a viscoelastic rod is excited by longitudinal harmonic waves in steady-state regime, its segments can be represented by "T" circuits where the elements are hyperbolic functions defined by the propagation constants and characteristic impedances, both of complex nature (Bacon and Brun, 2000). By combining the equations of input and transfer impedances, naturally introduced in the "T" topology, one obtains a global transfer matrix where the force and velocity fields in sections along the rod are mutually defined. In this work, the transfer matrices methodology is applied to simulate the propagation response in the PRDs, to convert the strain experimental signals in force and velocity signals by using spectral calculations and to determine the propagation response on the transducer face from the experimental signals measured at the monitoring points. The loading rods are designed to present a configuration where the impedance on the sensitive face of the transducer; i.e., the driving end impedance, can be considered satisfactorily close to the radiation impedance in the water at the transduction main frequency. For the whole half-power band of the transducer (43.5 kHz – 60.5 kHz), the accuracy criterion is to accept 5% as the maximum deviation between the analytical driving end impedance and the radiation impedance in the water.

Despite the 1-D nature of the dynamical equations in the matrices methodology, the coupled effects of the material and geometric dispersions can be partially considered in the analytical model by using the propagation and impedance parameters, both as function of the frequency and rod radius. Experimental results (Benatar et al., 2003; Tyas and Poppe, 2005) prove the good accuracy of such approach up to radius-wavelength ratios from which the longitudinal waves start to migrate to the rod surface, in a pattern that characterizes the propagation of Rayleigh waves. The solution can be based on propagation constant curves defined from the generalized Pochhammer equation (Pochhammer equation rewritten to treat viscoelastic materials) combined with an 1-D rheological model (Magalhães and Zindeluk, 2005) or, in a more conservative but not always feasible way, the curves may be determined by adopting experimental propagation methods (Lundberg and Blanc, 1988). Due to the satisfactory results obtained from the generalized Pochhammer equation and the high accuracy demonstrated by the rheological models of Zener (Sogabe and Tsuzuki, 1986) and Zhao (Zhao, 1992), when compared with experimental data published in the literature, semi-analytical propagation constants may be applied to design DUMILOAD rods. However, as summarized in the next section, a simplified characterization process, developed to obtain *in situ* the propagation constant curves in the loading rods, have been used to quantify the transmission response of the object transducer.

By modeling the transducer through the Finite Element/Boundary Element methods, the radiation impedance curve in the half-power band was defined taking into account the assembling conditions in the watertight hull. Such data were

applied in a recursive algorithm which led to the four different loading rod configurations indicated in Tab. 1. While the rods 1 and 2 were dimensioned considering material and geometric dispersions, for the rods 3 and 4 the effects of geometric dispersion were intentionally ignored, thus the latters were analytically assumed as bars. For 51 kHz, once the phase velocity defined in the 1-D dispersion model is 44% higher than the velocity calculated from the generalized Pocchammer equation, the diameter of the rods without geometric dispersion is lower than the rods where the double dispersive conditions are assumed. Also considering the main frequency, in view that 98% of the radiation impedance modulus are due to the resistive term, may be considered that one-diameter loading rods are able to acoustically simulate water. Notice that the rod segment coupled to the transducer face represents the reactive term and the other segment, longer than the first, simulates the acoustic radiation resistance. As summarized in Tab. 1, the deviations between the numerical value of hydroacoustic impedance and the analytical driving end impedance in the rods are lower than 3%.

Table 1: Dimensions and driving end input impedance of the Propagation Rod DUMILOADS.

Rod	Reactive segment diameter (mm)	Resistive segment diameter (mm)	Reactive/Resistive segments length (mm)	Driving end input impedance (Ns/m)	$\Delta R_r^{(1)}$ (%)	$\Delta X_r^{(2)}$ (%)
1	23.50	22.90	1.58/1798.42	794.536 + i 152.093	2.46	- 0.32
2	-	22.90	1800.00	772.717 + i 6.096	- 0.36	-
3	23.54	19.12	1.60/1798.40	798.414 + i 153.796	2.96	0.80
4	-	19.12	1800.00	776.103 + i 5.690	0.08	-

[1], [2] : deviations of the acoustic radiation resistance and acoustic radiation reactance in relation to the values defined by the FE/BE methods, for 51 kHz.

3. EXPERIMENTAL RESULTS

The apparatus shown in Fig. 2 was developed to carry out electrical imitance measurements and acoustical transmission tests in a Tonpilz transducer when loaded by a PRD. In the apparatus, some facilities allow adjustments between the main acoustic axis of the transducer and the longitudinal axis of the loading rods. With the aim to minimize eventual uncertainties when the results from the four PRDs are intercompared, rods 1-2 were machined by using a single raw part and rods 3-4 from another single one. To obtain the imitance curves, two methodologies were adopted: low intensity sinusoidal CW and high intensity tone bursts. As effect of the internal friction in the polymeric structure of the rods, the amplitude level of the CW excitation signals (1 Vp) was not high enough to generate eco signals on the transducer face. Such fact allowed the utilization of an Impedance Analyzer HP 4192A to calculate the imitance curves. However, in agreement with the excitation level applied during the acoustical transmission tests, the electrical imitance of the transducer was initially determined in response to tone bursts of 120 Vp. The congruency of the results obtained from the two types of excitation points out to the linear behavior of the measuring set.
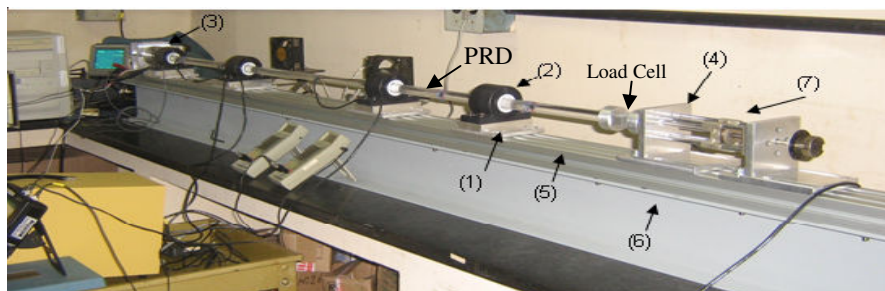

Figure 2. PRD apparatus: (1) bearing support, (2) sliding bearing, (3) transducer hull, (4) compression mechanism support, (5)"I" beam Rexroth AG 45x90, (6) "I" beam W150x13, (7) static compression mechanism.

Concerning the transmission tests, due to the very low thermal conductivity of the PMMA, the strain-gages used to monitor the calibrating waves could not be fed with a DC voltage high enough to establish a satisfactory signal-to-noise ratio (3.5 VDC was the highest voltage on the gages to maintain the electrical stability of the Wheatstone bridge). That is the reason the transducer was excited in the DUMILOAD by voltage amplitudes higher than adopted in the imitance and the in underwater acoustic tests. Based on the far field criterion and on criteria about the evanescent behavior of modes higher than the Young mode, monitoring points were established at 200, 450 and 900 mm from the transmission interface (points 1, 2 and 3). At such points, double rosette 90° strain-gages were used (MM CEA-13-125UT-350) in a full active Wheatstone bridge configuration. In terms of spectral resolution, the analytical cut-off frequencies of the gages are 77.5 and 132.0 kHz, respectively to the rods 1-2 and "bars" 3-4. In relation to the spatial resolution,

considering the analytical transduction frequency (51 kHz) and elements of length 3.18 mm, the highest strain measured by the gages is 1.7% lower than the true peak value of the signal. The gages were aligned on the longitudinal and circumferencial directions. To null the measurement of eventual bending strains, each pair of gages was fixed diametrically opposed to the other pair. During the transmission tests, the bridges were connected to a Signal Conditioner MicroMeasurements 2311, wired to a Digital Oscilloscope Tektronix THS710A and linked to an acquisition board inside a PC. The excitation system was basically composed of a Power Amplifier B&K 2713, a Function Generator HP 3314A and a Matching Transformer KH MT-56. To acoustically couple the transducer to the propagation rods the best results were obtained by using silicon gel. The experimental results herein presented reflect in laboratory measurements performed under temperature and moisture conditions varying up to 8 $^{\circ}$C and 10 %.

3.1. Electrical Imitance Measurements

Figure 3 shows the analytical and the experimental admittance curves on the transducer electrical terminals by loading effect of the rods 1 and 2, and the admittance curve of the transducer in a fresh water tank. As pointed out by the conductance curves in Fig. 3.a, the good agreement between the results proves that the rod 1 is close to simulate the hydroacoustic radiation resistance in the half-power band of the transducer. The peak value of the experimental curve obtained by using the rod 1 is only 1.8 % higher than the peak defined from the equivalent circuit model. In the DUMILOAD, the experimental and the analytical main frequencies of the transducer are respectively 52.2 and 51.5 kHz, thus diverging 1.4 %. Concerning the mechanical quality factor of the transducer in the rod, the proximity between the conductance curves leads to a discrepancy level lower than 16.0 %. Such results also denote that the resistive part of the radiation impedance in the driving end of the rod 1 can be regarded in accordance with the analytical one. On the other hand, based on the susceptance curves in Fig. 3.b, one may conclude that although the reactive segment of the rod 1 tends to improve the coupling condition in the transmission interface, its acoustical influence is not important enough to exactly represent the hydroacoustic radiation reactance. In relation to the experimental results defined in the rod 1 and in the water, the conductance peak of the transducer in the PRD is 11.7 % higher than the hydroacoustic peak.

As Fig. 3.c illustrates to the rod 2, the conductance peak in the DUMILOAD is about 8.1 % higher than the peak analytically predicted, although both curves indicate almost the same resonance frequency (divergence of 0.4%). In terms of experimental curves, the electrical conductance peak of the transducer in the rod 2 is 23.6 % higher than the peak in the water. Moreover, while in the PRD 2 the resonance frequency of the transducer is about 52.7 kHz, in the water the main resonance is verified at 51.2 kHz, so diverging 2.9 %. Such discrepancies are clearer in the susceptance curves, Fig. 3.d, and confirm that the reactive segment of the rod 1 does not entirely represent the inertial behavior of the hydroacoustic radiation impedance. Notice that the experimental reduction at the transduction frequency was only 500 Hz, and not 1.0 kHz as predicted by the model. In view that the transmission area between the object transducer and the rod 1 is 5.0 % bigger than the equivalent area in the rod 2, the results presented in Figs. 3.a and 3.b are more congruent than the results in Figs. 3.c and 3.d. However, it should be emphasized that the imitance results obtained from the rods 1 and 2 can be both considered satisfactory, especially when the uncertainties involved in the theoretical models and in the semi-analytical data applied for the rods designing are taken in account.

Figure 4 shows the admittance curves of the object transducer under the acoustical loading imposed by the rods or "bars" 3 and 4. As presumed, the results obtained from such media are worse than those ones defined by using rods 1 and 2. In relation to the conductance peak depicted in Fig. 4.a, the discrepancy between the experimental and analytical curves defined in the rod 3 is nearly 23.6 %. As well as the highest experimental conductance diverges 34.4 % of the value measured in the water, the profiles of the analytical and the experimental conductance curves are in clear disagreement. In this way, the mechanical quality factor of the testing transducer when loaded by the rod 3 is 31 % higher than the quality factor determined from the equivalent circuit. Otherwise, the difference is just 2.2 % in terms of resonance frequency. It is interesting to notice that two reasons are assumed as possible causes for the discrepancies verified in the rod 3: (1) the assumption of a bar materially dispersive without geometric dispersion lead to a rod configuration where the characteristic impedance values are in large disagreement with the water characteristic impedance, (2) the difference between the diameters of the reactive and the resistive rod segments, 4.42mm, may be enough to convert part of the acoustical energy transmitted by the transducer in strain work of the circular ring that distinguishes the two segments. In this sense, the reactive segment of the rod 3 is responsible by an inertial load that reduces in 500 Hz the transducer resonance frequency. The reduction theoretically presumed was nearly 1.5 kHz.

Figs. 4.c and 4.d show the admittance curves obtained through the tests with the rod 4. As the curves point out, the results are close to those defined in the rod 3. Despite the analytical assumptions adopted in the design of the loading rods, the imitance measurements lead to the conclusion that the "bars" 3 and 4 behave dynamically as rods.

3.2. Transmission Response Measurements

Initially, it is worthwhile analyzing two important aspects related to the processing of the experimental strain data obtained in the PRDs. As Magalhães and Zindeluk (2005) demonstrate, depending on the radius-wavelength ratio (a/Λ) associated with the wave components that effectively transmit the signal energy, the measurements on the rod perimeter can not be able to reflect the strain conditions throughout the cross-sections. It is well known that the smaller the

wavelength, the less homogeneous is the longitudinal displacement field and consequently the less plane is the disturbance. However, it is proved (Tyas and Poppe, 2005) that up to a/Λ near 0.32, the amplitude of the axial strain signal measured on the cylindrical surface of an elastic rod can be accurately corrected by multiplying the Fourier components by an averaging factor.
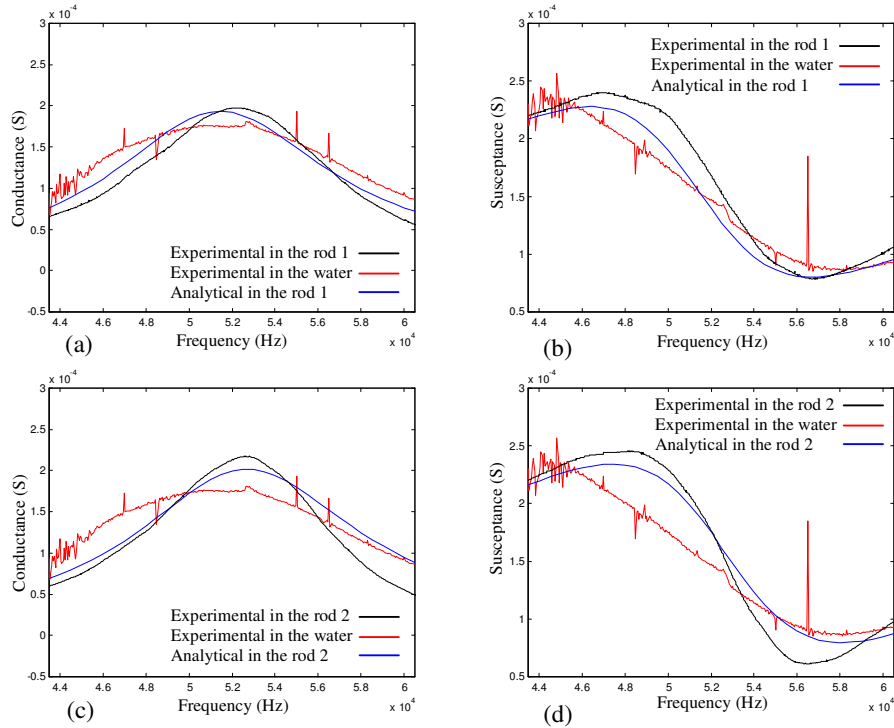

Figure 3. Analytical and experimental admittance curves of the testing transducer in the rods 1 and 2. Admittance curve of the transducer in the water.
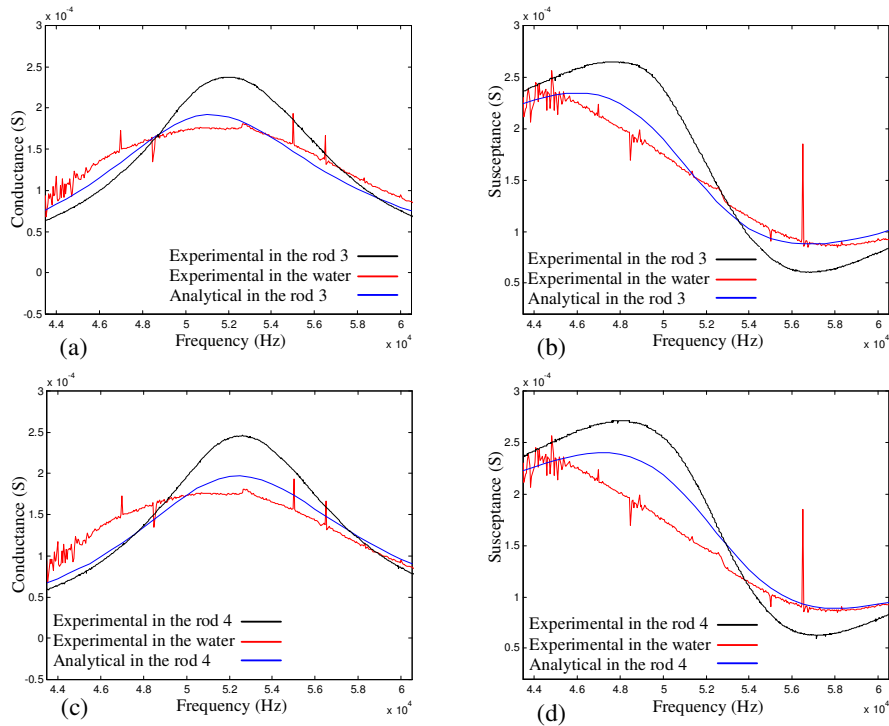

Figure 4. Analytical and experimental admittance curves of the testing transducer in the rods 3 and 4. Admittance curve of the transducer in the water.

In this sense, to mathematically compensate the cross-sectional non-planarity of longitudinal strain fields in rods made of linear viscoelastic polymers, Magalhães (2007) developed a closed-form equation which defines the averaging factor (correction factor) as function of the frequency or rod radius-wavelength ratio. Specifically for a PMMA rod, the solution of the equation establishes that the longitudinal strain on the cylindrical surface is zero for $a/\Lambda = 0.41$. By introducing in such equation the semi-analytical propagation constants applied to design the PRDs, it was obtained the critical frequencies for the longitudinal propagation process in the rods 1-2 and 3-4, respectively 54.5 kHz and 65.0 kHz. Once the longitudinal strain signal on the perimeter of the rods is practically non-existent at such frequencies, they were named cut-off frequency of the measuring process in a propagation rod.

Another aspect to be considered is the practical importance of characterizing *in situ* the loading rods. With this aim, it was developed an experimental methodology which defines the transfer functions of longitudinal strain signals along a polymeric rod under strong dispersive conditions and excited by tone bursts (Magalhães, 2007). Basically, for each frequency value in the interesting frequency band, the transfer function, and consequently the wavenumber and the attenuation factor, can be defined when such frequency is exactly the carrier component of the burst. In this way, the signal-to-noise ratio involved in the spectral calculations is able to be strongly optimized.

After preliminary transmission tests in the rods, it was verified that favorable propagation and measuring conditions could be obtained by exciting the object transducer with 50 cycles tone bursts, 0.35 - 0.50 seconds pulse rate, 32 samples averaging and 1.25 MHz sampling frequency. Concerning the rod 1, should be pointed out that for carrier frequencies above 56 kHz the strain signals measured at the point 1 (200 mm) present two different wave groups, the initial front group formed by cycles of longer wavelengths and the final rear group composed by shorter wavelengths, see Fig. 5. Such effect, which characterizes geometric dispersion in the rod, is superposed to a significant reduction in the signal amplitude for frequencies above about 54 kHz. In this case three probable causes are combined: reduction of the transmission response of the transducer above its fundamental resonance (52.2 kHz in the rod 1), increase of the material attenuation factor with the frequency rise and reduction of the signal amplitude on the rod perimeter for frequencies above the cut-off frequency. As expected, depending on the radius-wavelength ratio the reduction in the signal amplitude is not completely compensated by the correction factor. The normalized spectra in Fig. 6 demonstrate that the amplitude of the frequency components is significantly reduced for frequencies above 54.5 kHz and 65 kHz, respectively for the rods 1-2 and 3-4.
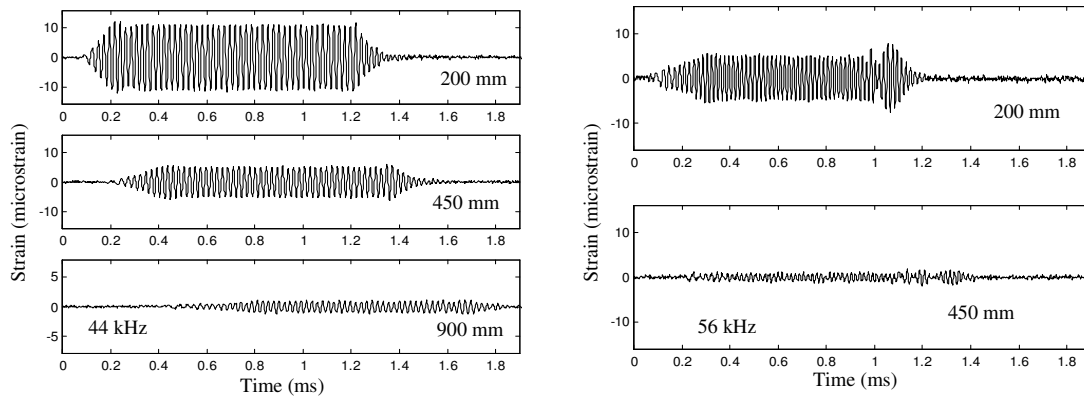

Figure 5. Strain signals in the rod 1. Transducer excitations for 44 kHz and 56 kHz - 77.25 Vrms and 76.19 Vrms.
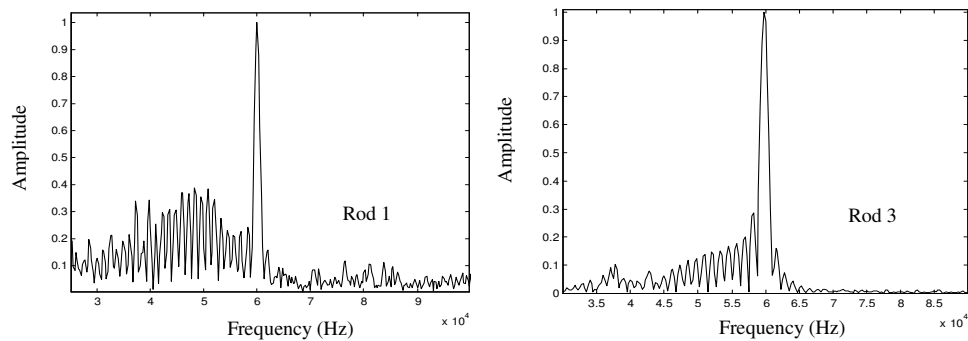

Figure 6. Normalized spectra of 60 kHz tone bursts in the rods 1 and 3.

To convert the strain signal in force and velocity signals, the semi-analytical propagation constant curves were mathematically adjusted by using the experimental propagation constant data obtained in the rods (Magalhães, 2007). This approach overcome some natural limitations of the material characterization methodology applied to the PRDs. Summarizing, in view that the signal-to-noise ratio of the experimental transfer functions is only satisfactory in the essential bandwidth (EBW), the out-band frequency components can not be used to define the acoustical characteristics of the propagation media over the entire frequency spectrum involved in the FFT and IFFT calculations.

With the aim to evaluate the accuracy of the analytical model developed for the PRDs, the experimental propagation constants were introduced in the electroacoustical equivalent circuit. The amplitude of the experimental signals was normalized by establishing 1 Vrms as an only voltage level applied to the transducer. In Fig. 7 are represented the curves analytically calculated from the experimental and from the semi-analytical propagation parameters, and the peak values of the force and velocity signals defined from the strain waves measured at the point 1. By comparing the force and velocity experimental curves with the analytical curves calculated by using experimental propagation constants, it is demonstrated the good accuracy of the propagation model for frequencies up to 53 kHz. In this case, the average deviation is about 3.7 %. Notice that for carrier frequencies above 53 kHz, thus from frequencies close to the cut-off frequency of the measuring process, the experimental results indicate the strong tendency of the disturbance in presenting a non-planar distribution. In addition, the considerable disagreement between the analytical curves calculated with the experimental parameters and defined from the semi-analytical propagation constants proves the high importance of characterizing *in situ* the PRDs, especially in relation to the attenuation factor.
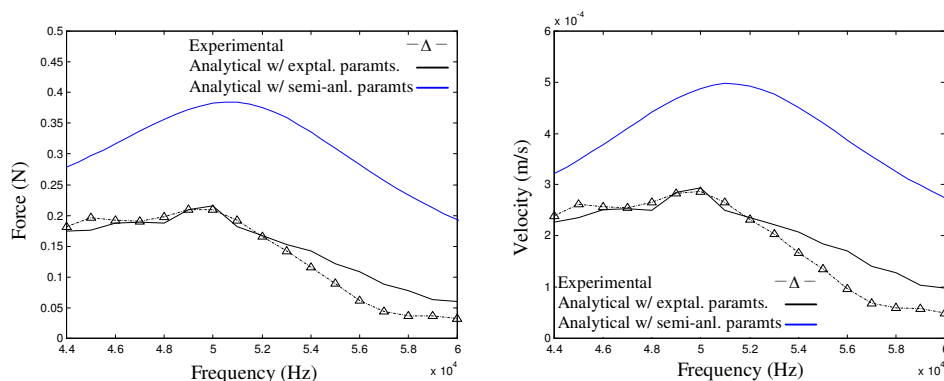

Figure 7. Force and velocity peaks at the point 1 of the rod 1, normalized for 1 Vrms. Experimental data, analytical curve with experimental propagation constants and analytical curve with semi-analytical propagation constants.

To define the transmission response of the transducer, the strain spectrum and, in consequence, the force and the velocity spectra are mathematically transferred from the measuring points to the transducer face. By using the signals amplitude in the time-domain, the average power and the transmission level of the acoustical source can be both calculated. For the rod 1, Fig. 8 shows examples of strain signals measured at the point 1 and after being transferred to the sensitive face of the transducer. Concerning the 53 kHz pulse, it is clear the good effect of the dispersion correction method on the distortions observed along the transient intervals. In that signal, not only a few distorted peaks in the final portion of the burst are corrected when transferred to the transducer face, but also the profile of the translated signal becomes identical to the profile of the electrical current signal which characterizes the transducer when it is excited close to the main resonance. On the other hand, as Fig. 8 also indicates, the transfer function does not demonstrate a good performance to correct the geometric dispersion effects in the 57 kHz burst. Probably this limitation is due to the low amplitude of the strain signal on the rod surface at such frequency, leading to an insufficient signal-to-noise ratio.

In Fig. 9 are depicted the analytical and the experimental peaks of force and velocity on the transducer face by loading effect of the rod 1. From both diagrams it is possible to verify that up to 53 kHz the analytical curves are close to the experimental ones. Taking into account the force curves, it is interesting to notice that the discrepancies between the two analytical results are not important up to 53 kHz. At the measuring point 1 such good agreement is not observed due to the significant difference between the semi-analytical and the experimental attenuation factors. Equally for the rod 1, the data represented in Fig. 9 lead to the average acoustic power on the transducer face. The profiles of the analytical and experimental power curves are almost similar to the curves in Fig. 9, with an average deviation of about 7.0 % from 43.5 kHz up to 53 kHz (Magalhães, 2007). Based on such curves, one can obtain the acoustic transmission level of the testing transducer under more rigorous assumptions that usually found in the literature. In this sense, the transmission response curves shown in this paper were determined by algebraically reducing the sound level equation of sonar transducers in order to parameterize the terms of directivity index and characteristic impedance.

In this way, in Fig. 10.a the analytical and the experimental transmission responses of the transducer in the <u>rod 1</u> are represented with the hydroacoustic transmission response. As expected, the absolute calibration process in such rod is limited up to around 53 kHz, from which the discrepancies between the curves become significant. Equally considering this frequency limit, the highest deviation between the analytical and the experimental curves in the rod 1 is 0.9 dB. By comparing the hydroacoustic transmission curve with the practical response curve in the DUMILOAD, it can be verified that the deviation rises to about 1.1 dB. Such variations are in accordance with the tolerance limits recommended by the ANSI standard (1988). Therefore, likewise the electrical imitance tests, the transmission response measurements prove that the radiation behavior of the PRD 1 is close to the behavior analytically defined in the design stage and close to the acoustic radiation in the water.
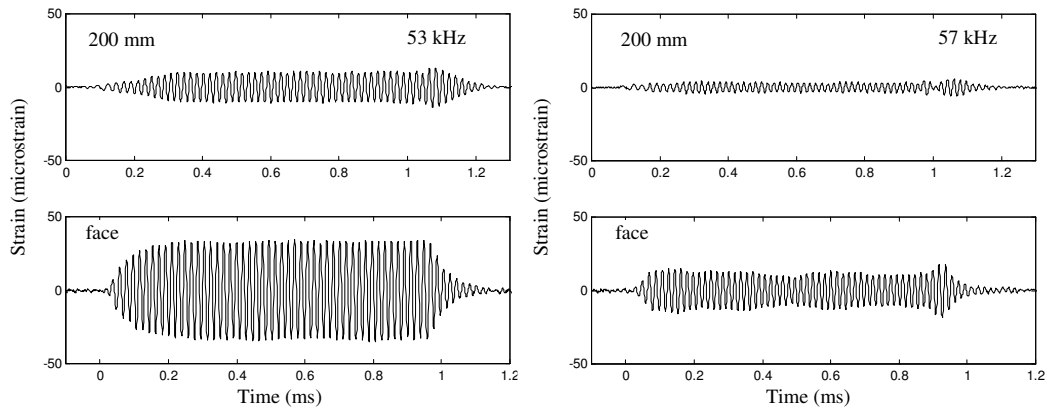

Figure 8. Strain signals at the point 1 of the rod 1 and transferred to the transducer face. Transducer excitations for 53Hz and 57kHz – 76.54 Vrms and 76.23 Vrms.
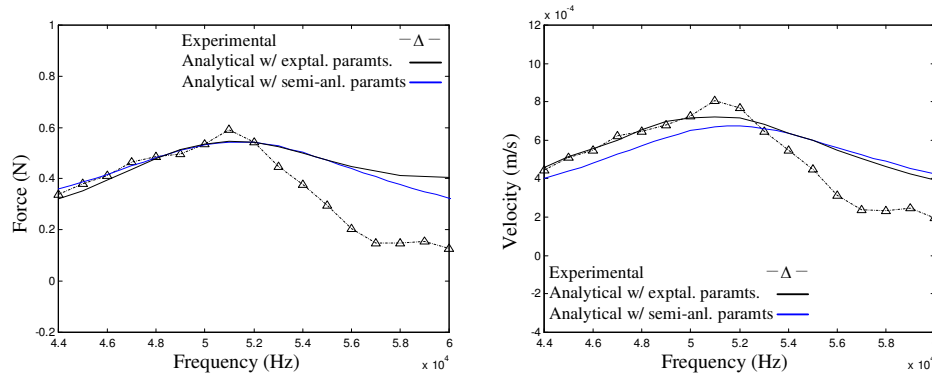

Figure 9. Force and velocity peaks on the transducer face by loading effect of the rod 1, normalized for 1 Vrms. Experimental data, analytical curve with experimental propagation constants and analytical curve with semi-analytical propagation constants.

Figure 10.b shows the transmission response curves of the object transducer by loading effect of the <u>rod 2</u>. When compared with the experimental results obtained in the rod 1, the experimental transmission curve in the DUMILOAD confirms the lower capacity of the rod 2 to simulate the hydroacoustic radiation impedance. Moreover, the results defined in the rod 2 vary more with the frequency than in the rod 1. As mentioned before, such worse performance is probably due to the difference between the transmission surfaces of the two rods. In quantitative terms, the highest discrepancy between the experimental results in the rod and in the water is nearly 2.0 dB, up to 53 kHz. In turn, 1.8 dB is the highest deviation between the analytical curve calculated with experimental parameters and the experimental curve defined from the strain measurements in the PRD 2. However, taking into account the amount of uncertainty factors related to the acoustic propagation in a double dispersive medium, one can consider that the inaccuracy of the experimental results in the rod 2 does not make it unfeasible to be used as an absolute calibration device. Thus, once assumed that the electrical imitance by using the rod 2 are sufficiently close to the experimental imitance of the transducer in the water, the discrepancies between the transmission responses in the two acoustic media may be compensated being adopted some practical procedures, such as the simple addition of a gain factor.

In Fig. 10.c are shown the analytical and the experimental transmission curves of the transducer in the <u>rod 3</u> and in the water. In terms of amplitude the results do not present the same good agreement verified for the rods 1 and 2.

However, should be remarked the good agreement between the profiles of the analytical and experimental curves in the PRD 3. Such congruence is probably due to the fact that the cut-off frequency of the measuring process in the rod 3 is above the highest frequency of the half-power band of the object transducer. At least in qualitative terms, the results point out to the importance of having the strain signals in an undistorted condition and of obtaining a satisfactory signal-to-noise ratio. The causes for the inaccuracy of the transmission measurements in the rod 3 are the same ones assumed for the imitance measurements. Concerning the confrontation between the analytical and the experimental results in the DUMILOAD, the highest deviation is about 3.1 dB over the entire half-power band. The disagreement between the experimental results in the rod and in the water is 6.3 dB. However, considering frequencies up to 53 kHz the highest deviation is 3.2 dB.

At last, as seen in Fig. 10.d, in terms of amplitude there are a few discrepancies between the transmission curves obtained in the rods 3 and 4. In the rod 4, the highest deviation between the analytical and the experimental curves in the DUMILOAD is 5.7 dB. Considering the experimental data in the water and in the rod 4, the highest disagreement is about 6.5 dB. For frequencies up to 53 kHz the results diverge 3.9 dB. Therefore, as presumed from the imitance measurements, the rods 3 and 4 do not satisfactorily simulate the hydroacoustic loading conditions for the testing transducer. However, in view that the geometric dispersion effects in such rods are only significant for frequencies above the calibration band, it might be admissible to correct the transmission curves obtained in the DUMILOAD by comparing them with the transmission curve of a standard transducer.
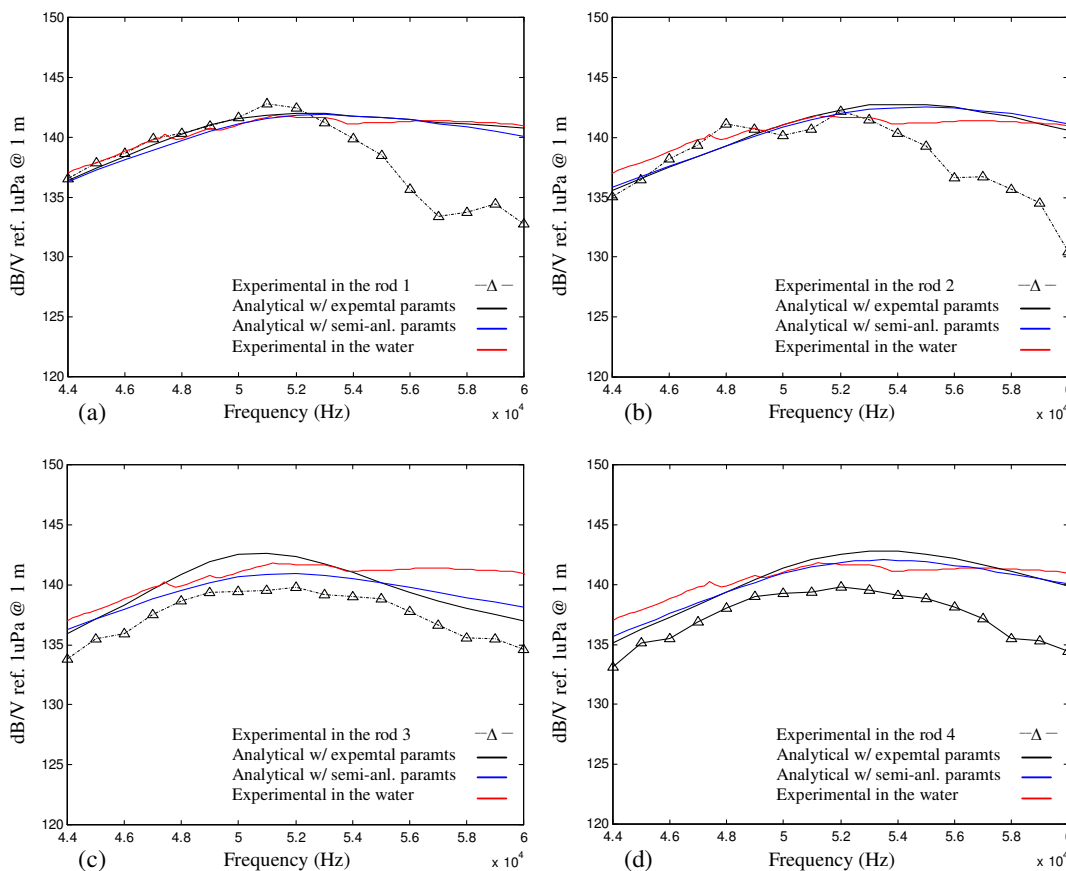

Figure 10. Experimental transmission response curves in the water and in the rods 1 (a), 2 (b), 3 (c) and 4 (d). Analytical curve with experimental propagation constants and analytical curve with semi-analytical propagation constants.

4. CONCLUSIONS

This work synthesizes some of the main experimental results obtained in a novel type of dummy mechanical impedance load, named "Propagation Rod DUMILOAD", which has been developed to simulate the hydroacoustic impedance to a Tonpilz transducer. Since the device uses a PMMA rod as longitudinal propagation medium, the transmission of axial acoustic waves is invariably submitted to the effects of material dispersion and, depending on the radial inertia influence, also submitted to the geometric dispersion effects. Such dispersions can be partially introduced in the propagation model by using the characteristic impedances and propagation constants defined from the coupling of

1-D rheological models and the Pochhammer generalized solution for linear viscoelastic rods. The good agreement between the semi-analytical propagation constants and experimental data published in the literature led to the design of four DUMILOAD rods. With the aim to model the propagation behavior, a matrix transfer method was applied to define the electrical imitance curves on the transducer terminals and to obtain its transmission response along the rods.

As commented in the paper, depending on the rod radius-wavelength ratio the signal extracted by strain-gages on the rod surface is not able to represent the conditions throughout the cross-sections. In this sense, the non-planar characteristics of the disturbance could be minimized by adopting double rosette strain-gages and by applying a correction factor for the amplitude of the Fourier components. Based on comparisons between the analytical and experimental results in the PRDs, important characteristic frequencies associated with the propagation phenomenon in double dispersive acoustic media were identified. It is shown that, above a particular frequency, the amplitude of the strain signals in a PRD decreases to inappropriate levels. Such frequency is named "cut-off frequency of the measuring process". To overcome this limitation, in a future step propagation rods shall be designed with the driving end impedance centered at frequency values distributed over the whole range of interest.

The experimental results obtained in the imitance tests, and especially the results defined from the transmission measurements, prove the good capacity of the propagation model to predict the longitudinal response of acoustic rods under moderate dispersion conditions. The results also point out to the real convenience of characterizing *in situ* the acoustical properties of the PRDs. The experimental propagation constants were successfully applied to convert the strain signals in force and velocity signals. Furthermore, good results were also obtained with the mathematical transference of the strain signals from the measuring points to the sensitive face of the transducer, once the amplitude and phase distortions of the longitudinal disturbances were satisfactorily corrected up to the cut-off frequency of the measuring process.

Specifically concerning the PRDs analyzed in this work, one can conclude that, in acoustic terms, the rods 1 and 2 represent water to the testing transducer. The rods 3 and 4 introduce significant errors in the imitance measurements and so can not be used for endurance tests. Moreover, while the absolute calibration process can be directly applied for the rods 1 and 2, for the rods 3 and 4 may be adopted a calibration procedure where the transmission response in the DUMILOAD would be compensated by using the transmission curve of a standard transducer. In an overview, the type of DUMILOAD here proposed presents some advantages in relation to fresh water tanks and hydrostatic anechoic chambers; such as, more economical conditions, non-problematic access to the internal parts of the transducer during the calibration measurements, control of the temperature and moisture conditions and natural simplicity for testing a big amount of transducer elements.

5. REFERENCES

Afonso, O.J.R. and Magalhães, F.L., 1999, "Development of a Mechanical Impedance Technique for High Power Performance Tests of Hydroacoustic Transducer in Air", Proceedings of the 15th Brazilian Congress of Mechanical Engineering, CD-ROM, Águas de Lindóia, Brazil.

American National Standard, 1988, "Procedures for Calibration of Underwater Electroacoustic Transducers", ANSI S1.20-1988, New York, USA, 38 p.

Bacon, C. and Brun, A., 2000, "Methodology for a Hopkinson Test with a Non-Uniform Viscoelastic Bar", International Journal of Impact Engineering, Vol.24, pp. 219-230.

Benatar, A., Rittel, D. and Yarin, A.L., 2003, "Theoretical and Experimental Analysis of Longitudinal Wave Propagation in Cylindrical Viscoelastic Rods", Journal of the Mechanics and Physics of Solids, Vol.51, No. 8, pp. 1413-1431.

Casem, D.T., Fourney, W. and Chang, P., 2003, "Wave Separation in Viscoelastic Pressure Bars Using Single-Point Measurements of Strain and Velocity", Polymer Testing, Vol.22, pp.155-164.

Lundberg, B. and Blanc, R.H., 1988, "Determination of Mechanical Material Properties from the Two-Point Response of an Impacted Linearly Viscoelastic Rod Specimen", Journal of Sound and Vibration, Vol.126, pp. 97-108.

Magalhães, F.L. and Zindeluk, M., 2005, "Material and Geometric Dispersions in a DUMILOAD for Sonar Transducers", Proceedings of the 18th International Congress of Mechanical Engineering, CD-ROM, Ouro Preto, Brazil.

Magalhães, F.L., 2007, "Acoustic Loading Device for Testing Underwater Acoustic Transducers in the Air: Propagation Rod DUMILOAD", D.Sc. thesis (in Portuguese), COPPE/UFRJ, Rio de Janeiro, Brazil, 311 p.

Sogabe, Y. and Tsuzuki, M., 1986, "Identification of the Dynamic Properties of Linear Viscoelastic Materials by the Wave Propagation Testing", Bulletin of JSME, Vol.254, pp.2410-2417.

Tyas, A. and Poppe, D., 2005, "Full Correction of First-Mode Pochhammer-Chree Dispersion Effects in Experimental Pressure Bar Signals", Measurements Science and Technology, Vol.16, pp. 642-652.

Xiping, H. and Jing, H., 2009, "Study on the Broadband Tonpilz Transducer with a Single Hole", Ultrasonics, Vol.49, No. 4-5, pp. 419-423.

Zhao, H., 1992, "Analyse de l'essai aux Barres d'Hopkinson – Application à la Mesure du Comportement Dynamique des Matériaux", Ph.D. thesis (in French), Ecole Polytechnique du Paris - ENPC, Paris, France.

6. RESPONSIBILITY NOTICE

The authors are the only responsible for the printed material included in this paper.